Population Balance Modeling for a Continuous Gas Phase Olefin Polymerization Reactor

KYU YONG CHOI,* XIA ZHAO, and SHIHUA TANG

Department of Chemical Engineering, University of Maryland, College Park, Maryland 20742

SYNOPSIS

Steady-state population balance models have been developed for a continuous flow gas phase olefin polymerization process with both uniform sized and log-normally size distributed high activity catalyst feeds. For the calculation of polymer properties such as molecular weight averages and weight fraction of comonomers in the copolymer, a multigrain solid core model was used with an assumption that intraparticle monomer mass transfer resistance is negligibly small. The multigrain solid core model was incorporated into the population balance model and the effects of feed catalyst particle size distribution and catalyst deactivation parameters on the polymer production rate, polymer particle size distribution, and polymer properties were investigated. It is observed for deactivating catalyst that the polymer particle size distribution tends to be narrower with a reduced amount of large polymer particles. For the catalyst with nonuniform site deactivation, polymer particles of different sizes exhibit different molecular weight and copolymer composition. © 1994 John Wiley & Sons, Inc.

INTRODUCTION

High and low density olefin polymers (e.g., HDPE, LDPE, LLDPE, PP, etc.) are manufactured commercially using transition metal catalysts or Ziegler-type catalysts in liquid slurry or gas phase polymerization reactors. In continuous gas phase olefin polymerization processes, both fluidized bed reactors and mechanically stirred bed reactors are widely used. Quite often, it is desirable to control the average size or size distribution of polymer particles. This is because average particle diameter, particle size distribution, fines content, shape, bulk density, surface roughness, and porosity may affect the polymerization rate and the dispersion and mixing of additives in the finishing stage. If polymer particle size or size distribution can be controlled properly, one can eliminate costly pelletization steps. When polymers are produced in a continuous flow reactor, the size of a polymer particle or its size distribution is determined by its age or age distribution in the reactor. If the polymers of different sizes exhibit different properties (e.g., molecular weight, molecular weight distribution, density, etc.), knowing the polymer particle size distribution is important because the overall polymer properties are the average values of individual polymer particles of different sizes.

In this article we present the population balance models for a continuous flow ethylene copolymerization reactor operating at steady state. The effects of feed catalyst particle size and catalyst deactivation characteristics on the polymer properties and particle size distribution are investigated through model simulations.

POLYMERIZATION IN A SINGLE POLYMER PARTICLE

One of the unique features of heterogeneously catalyzed olefin polymerization processes is the breakup of highly active initial catalyst particles shortly after initiation, followed by a buildup of polymer layer around the catalyst particles. After the breakup of the original catalyst particle, each catalyst fragment

* To whom correspondence should be addressed.

Journal of Applied Polymer Science, Vol. 53, 1589–1597 (1994)
 CCC 0021-8995/94/121589-09

becomes loosely connected by polymers to other catalyst fragments. The catalyst–polymer particle then grows to a larger size as the reaction continues. There is a possibility that intraparticle mass transfer resistance may increase as a polymer particle grows. The modeling of a growing catalyst–polymer particle in transition metal catalyzed olefin polymerization processes has been studied extensively by Taylor and coworkers.[1] Using a complex but realistic multigrain model, they report that both intraparticle and interfacial monomer mass transfer limitations can cause a reduced overall polymerization rate and a broadening of molecular weight distribution in heterogeneously catalyzed propylene and ethylene polymerizations. They also report that the existence of multiple active catalytic sites of differing polymerization activity may also cause the broadening of polymer molecular weight distribution, as suggested by other researchers. Kakugo et al.[2,3] carried out scanning electron microscopy and X-ray microanalysis of the polyolefin particles and reported that a polymer particle (d_p of about 800–1,000 μm) consists of small microparticles (d_p of about 0.1–0.35 μm) that contain one or two catalyst crystallites (d_p of about 50–170 Å). Kakugo and coworkers' observation[2,3] is in close agreement with the multigrain model structure proposed by Taylor et al.[1]

Recently, it has been pointed out by Hutchinson and Ray[4] that equilibrium sorption also plays an important role in determining the local concentration of monomers in the solid polymer phase. In other words, the thermodynamics of monomer sorption in semicrystalline polyolefins control the monomer accessability to the catalyst surface, and thus the polymerization rate. For example, when ethylene is copolymerized with higher α-olefin comonomers in gas phase polymerization, the local concentration of comonomer in the solid phase can be higher than in the bulk gas phase. This theory provides a qualitative understanding of some unusual rate enhancement phenomena observed in some ethylene polymerizations with olefin comonomers such as butene-1 or hexene-1.

If the intraparticle monomer diffusion resistance is negligibly small, one can assume that each microparticle containing a transition metal crystallite will grow to an equal size particle. This implies that the growth of a macroparticle can be modeled as a growth of an assemblage of equal sized microparticles. Then, all we need to know to calculate the size of a macroparticle is the initial catalyst particle size and the size of the catalyst crystallite after the breakup. If each catalyst particle is assumed spherical and the size of the catalyst crystallite after the breakup is uniform, the total number of microparticles in a macroparticle can be easily calculated. We name this simplified multigrain model as the multigrain solid core model (MGSCM). Figure 1 is the schematic diagram of the MGSCM. One major advantage of using this simplified polymer particle model is that it can be easily incorporated into a population balance reactor model in which the residence time history of every polymer particle must be followed. The molecular weight properties and composition of each polymer particle are calculated using the MGSCM and then the properties of these particles are integrated over the whole particle size range to obtain the overall properties of a polymer particle mixture.

DEVELOPMENT OF A POPULATION BALANCE MODEL

Let us consider a perfectly backmixed, continuous flow, stirred gas phase ethylene copolymerization reactor operating at steady state. A small amount of preactivated high activity catalyst is supplied to the reactor with the injection rate of F_0 (g/h). The particle mixing can be accomplished by a mechanical stirrer (stirred bed reactor) or high velocity feed gas (fluidized bed reactor). The reactor volume or bed weight (W_b) is kept constant by regulating the polymer withdrawal rate. Ethylene (M_1) and comonomer (M_2), hydrogen, and inert gas are fed to the reactor at a constant flow rate. We assume that no catalyst particles are lost by entrainment and the reactor is operated isothermally. The reactions to be considered in our copolymerization reaction modeling are shown in Table I. In this kinetic scheme, we assume that hydrogen chain transfer reaction is the main chain transfer reaction that affects the polymer molecular weight under isothermal reaction conditions. Thus, neither chain transfer to monomers nor spontaneous chain transfer reactions are considered in the kinetic model.

In our modeling, we shall consider both uniform sized feed catalyst particles and log-normally distributed feed catalyst particles that grow to larger polymer particles. In deriving the steady-state population balance model for a continuous gas phase polymerization reactor in which polymer particles grow, we take the modeling approach proposed by Kunii and Levenspiel.[5] It should be pointed out that unlike the fluidized bed reactor systems used in the process industry where gaseous components are usually the major products of interest, the solid

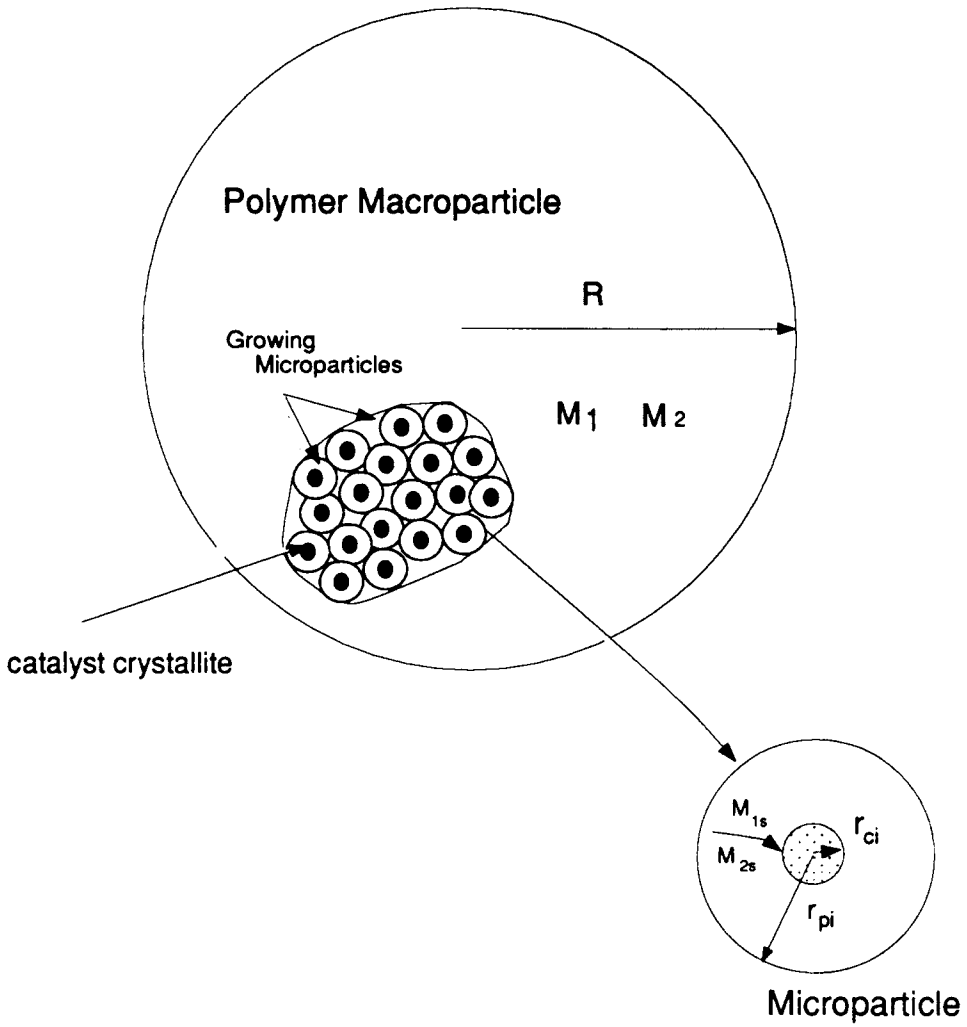

Figure 1 Multigrain solid core model.

phase itself is the reaction product in gas phase fluidized bed olefin polymerization processes.

For uniform sized catalyst feed particles, the steady-state population balance model equation takes the following form:

Table I Kinetic Scheme for Copolymerization

Initiation	$C^* + M_1 \xrightarrow[k_{i2}]{k_1} P_{1,0}$
	$C^* + M_2 \xrightarrow{k_{11}} Q_{0,1}$
Propagation	$P_{n,m} + M_1 \xrightarrow{k_{12}} P_{n+1,m}$
	$P_{n,m} + M_2 \xrightarrow{k_{21}} Q_{n,m+1}$
	$Q_{n,m} + M_1 \xrightarrow{k_{22}} P_{n+1,m}$
	$Q_{n,m} + M_2 \xrightarrow{k_{f1H_2}} Q_{n,m+1}$
Chain transfer	$P_{n,m} + H_2 \xrightarrow[k_{f2H_2}]{} M_{n,m} + C^*$
	$Q_{n,m} + H_2 \xrightarrow{k_{dc}} M_{n,m} + C^*$
Catalyst deactivation	$C^* \xrightarrow{k_{d1}} D^*$
	$P_{n,m} \xrightarrow{k_{d2}} M_{n,m} + D^*$
	$Q_{n,m} \rightarrow M_{n,m} + D^*$

$$F_0 p_0(R) - F_1 p_1(R) - W_b \frac{d[\Psi(R) p_1(R)]}{dR} + \frac{3W_b}{R} \Psi(R) p_1(R) = 0 \quad (1)$$

where $p_1(R)dR$ is the volume fraction of particles of size between R and $R + dR$; $\Psi(R)$ is the rate of particle growth for a particle of radius R (i.e., $\Psi(R) = dR/dt$); F_1 is the polymer production rate; F_0 the catalyst injection rate; W_b the solid bed weight; and R_i the initial catalyst particle radius. For uniform sized feed catalyst of radius R_i, there are no polymer particles of radius smaller than R_i. The mass balance for the catalyst particles is given as

$$F_0 - W_b \Psi(R_i) p_1(R_i) = 0. \quad (2)$$

Then, Eq. (1) is solved to yield

$$p_1(R) = \frac{F_0}{W_b\Psi(R)}\frac{R^3}{R_i^3} \times \exp\left(-\int_{R_i}^{R}\frac{F_1}{W_b\Psi(R)}\,dR\right). \quad (3)$$

Because the particle size is a measure of the reaction time or the particle's age in the reactor, the above equation can also be expressed as follows:

$$p_1(R) = \frac{F_0}{W_b\Psi(R)}\frac{R^3}{R_i^3}\exp\left(-\frac{F_1}{W_b}t(R)\right) \quad (4)$$

where $t(R)$ is the time for the catalyst particle to grow from radius R_i to R. Because $\int_{R_i}^{R_{max}} p_1(R)\,dR = 1$, Eq. (4) is integrated to yield

$$\frac{W_bR_i^3}{F_0} = \int_{R_i}^{R_{max}}\frac{R^3}{\Psi(R)}\exp\left(-\frac{F_1}{W_b}t(R)\right)dR. \quad (5)$$

Here, the overall rate of copolymerization in a macroparticle is given by

$$R_p = (k_{11}P + k_{21}Q)M_{1s} + (k_{12}P + k_{22}Q)M_{2s} \quad (6)$$

where, P and Q denote the total concentrations of live polymer chains with M_1 and M_2 attached to active sites, respectively. The monomer concentrations at the catalytic surface are obtained by solving the steady-state mass balance equations for the microparticle:

$$M_{1s} = \frac{\eta_1 M_{1b}}{1 + (k_{11}P + k_{21}Q)\rho_c r_{ci}^2\left(1 - \frac{r_{ci}}{r_{pi}}\right)\Big/ 3D_{s1}} \quad (7a)$$

$$M_{2s} = \frac{\eta_2 M_{2b}}{1 + (k_{12}P + k_{22}Q)\rho_c r_{ci}^2\left(1 - \frac{r_{ci}}{r_{pi}}\right)\Big/ 3D_{s2}} \quad (7b)$$

where η_1 and η_2 are the sorption factors for ethylene and comonomer[4] ($\eta_1 = M_1/M_{1b}$, $\eta_2 = M_2/M_{2b}$); P and Q are the total concentrations of $P_{n,m}$ and $Q_{n,m}$-type live polymers; M_{1b} and M_{2b} the bulk phase concentrations of ethylene and comonomer; ρ_c the catalyst density; D_{sj} the diffusivity of component j; r_{ci} the radius of catalyst crystallite; and r_{pi} is the radius of the growing microparticle. For the microparticles, the effect of monomer diffusion resistance has been found very small with the catalyst parameters and reaction conditions used in our study.

If the bed weight (W_b) is fixed, the particle growth rate $\Psi(R)$ and the time $t(R)$ needed for a particle to grow from a given initial size R can be obtained by solving the MGSCM. Then, the polymer production rate F_1 (kg/h) needs to be determined by solving Eq. (5). Because the polymer particle growth rate is given by

$$\Psi(R) = \frac{R_i^3}{3(1-\epsilon)R^2}\frac{\rho_c}{\rho_p}R_p \quad (8)$$

where R_p is the rate of polymerization (g-polymer/g-catalyst.h), Eq. (5) is reduced to

$$\frac{W_bR_i^6}{3(1-\epsilon)F_0} = \int_{R_i}^{R_{max}}\frac{\rho_p}{\rho_cR_p}R^5 \times \exp\left(-\frac{F_1}{W_b}t(R)\right)dR. \quad (9)$$

Here, ϵ is the particle voidage, ρ_p and ρ_c are the polymer particle density and catalyst density, respectively. The particle size distribution is also given as

$$p_1(R) = \frac{3(1-\epsilon)F_0R^5}{W_bR_i^6}\frac{\rho_p}{\rho_cR_p} \times \exp\left(-\frac{F_1}{W_b}t(R)\right). \quad (10)$$

In the above, the population balance model has been derived for a catalyst feed of uniform particle size. In practice, however, the feed catalyst particles may comprise the catalyst particles of different sizes (e.g., supported catalysts). In such a case, the steady-state population balance model is modified as follows. In the product stream, the solids of size R consist of particles grown from different initial sizes, that is,

Table II Standard Simulation Conditions ($C_2^=/C_4^=$)

Parameters	Value
Reaction pressure	35 atm
Reaction temperature	80°C (353 K)
Reactor bed weight	150 kg
Catalyst injection rate	5.0 g/h
Initial catalyst diameter	50.0 μm
Microcatalyst particle diameter	0.01 μm
M_2/M_1 in feed gas	0.2
N_2 in feed gas	40%
H_2 concentration	0.01 mol/L

$$p_1(R) = \int_{R_m}^{R} p_1(R, R_i) p_0(R_i)\, dR_i \qquad (11)$$

where R_m is the smallest catalyst particle size in the feed that grows to size R; $p_1(R, R_i)$ is the fraction of particles of radius R grown from the catalyst particle of size R_i; and $p_0(R_i)$ is the fraction of particles of size R_i in the catalyst feed. Then, the overall steady-state population balance equation takes the following form[7]:

$$\frac{W_b \rho_c}{3(1-\epsilon)F_0} = \int_{R_m}^{R_{max}} \int_{R_m}^{R} \frac{\rho_p R^5}{R_p R_i^6} \times \exp\left(-\frac{F_1}{W_b} t(R)\right) p_0(R_i)\, dR_i\, dR. \qquad (12)$$

The polymer particle size distribution is given as

$$p_1(R) = \frac{3(1-\epsilon)F_0}{W_b} \int_{R_m}^{R} \frac{\rho_p R^5}{\rho_c R_p R_i^6} \times \exp\left(-\frac{F_1}{W_b} t(R)\right) p_0(R_i)\, dR_i. \qquad (13)$$

Equations (9)–(10) and (12)–(13) are solved for the polymer production rate, F_1, by the iterative method.[5,6] The average particle residence time in the reactor is then calculated by

$$\theta = \frac{W_b}{F_1}. \qquad (14)$$

The average properties of polymer particles of size R grown from different initial catalyst particle sizes can be calculated using the following equations:

$$M_n(R) = \frac{\int_{R_{m,e}}^{R_{i,max}} M_n(R, R_i) p_0(R_i)\, dR_i}{\int_{R_{m,e}}^{R_{i,max}} p_0(R_i)\, dR_i} \qquad (15a)$$

$$M_w(R) = \frac{\int_{R_{m,e}}^{R_{i,max}} M_w(R, R_i) p_0(R_i)\, dR_i}{\int_{R_{m,e}}^{R_{i,max}} p_0(R_i)\, dR_i} \qquad (15b)$$

$$C_x(R) = \frac{\int_{R_{m,e}}^{R_{i,max}} C_x(R, R_i) W_p(R, R_i) \times p_0(R_i)\, dR_i}{\int_{R_{m,e}}^{R_{i,max}} W_p(R, R_i) p_0(R_i)\, dR_i} \qquad (15c)$$

$$R_p(R) = \frac{\int_{R_{m,e}}^{R_{i,max}} R_p(R, R_i) p_0(R_i)\, dR_i}{\int_{R_{m,e}}^{R_{i,max}} p_0(R_i)\, dR_i} \qquad (15d)$$

where $W_p(R, R_i)$ is the weight of polymer particles of radius R grown from size R_i; $R_{m,e}$ is the radius of the smallest catalyst particle that grows to size R; and $C_x(R)$ is the weight fraction of comonomer in the polymer particle of radius R. It should be pointed out that in general, $R_{m,e}$ is not equal to R_m. For example, for deactivating catalyst, the smallest catalyst particle may never grow to a certain size polymer particle, say R. $M_n(R)$ [M_w] is the number (weight) average molecular weight of a polymer particle of radius R and R_p is the polymerization rate in a particle of radius R. Once the properties of a polymer particle of given size are computed using the above equations, the overall properties of a whole polymer particle mixture withdrawn from the reactor are calculated by integrating these properties for all the particles of different sizes. The polymer molecular weight can be easily calculated using the molecular weight moments as described in Ray.[7] The moment equations for both live and dead polymers are solved together with the mass balance equations for ethylene, comonomer, and hydrogen.

RESULTS AND DISCUSSION

The steady-state population balance models presented in the above have been solved for the ethylene–butene-1 copolymerization system using the standard reaction conditions shown in Table II. The kinetic constants used in the model simulation are shown in Table III. The catalyst considered in this work is known to deactivate during the course of polymerization. Thus, the effect of catalyst site deactivation on the polymer particle size distribution is first studied and the model simulation results are shown in Figure 2 for both (a) nondeactivating catalyst and (b) deactivating catalyst. Here, the cata-

Table III Kinetic Constants ($C_2^=/C_4^=$)

$k_{11} = 7.524 \times 10^9 \cdot \exp(-7000/RT)$ L/mol·h
$k_{12} = 2.513 \times 10^8 \cdot \exp(-7000/RT)$ L/mol·h
$k_{21} = 7.524 \times 10^8 \cdot \exp(-7000/RT)$ L/mol·h
$k_{22} = 1.004 \times 10^8 \cdot \exp(-7000/RT)$ L/mol·h
$k_{f1H_2} = 1.626 \times 10^8 \cdot \exp(-8000/RT)$ (L/mol)$^{1/2}$/h
$k_{f2H_2} = k_{f1H_2}$

Constants from Hutchinson and Ray.[4]

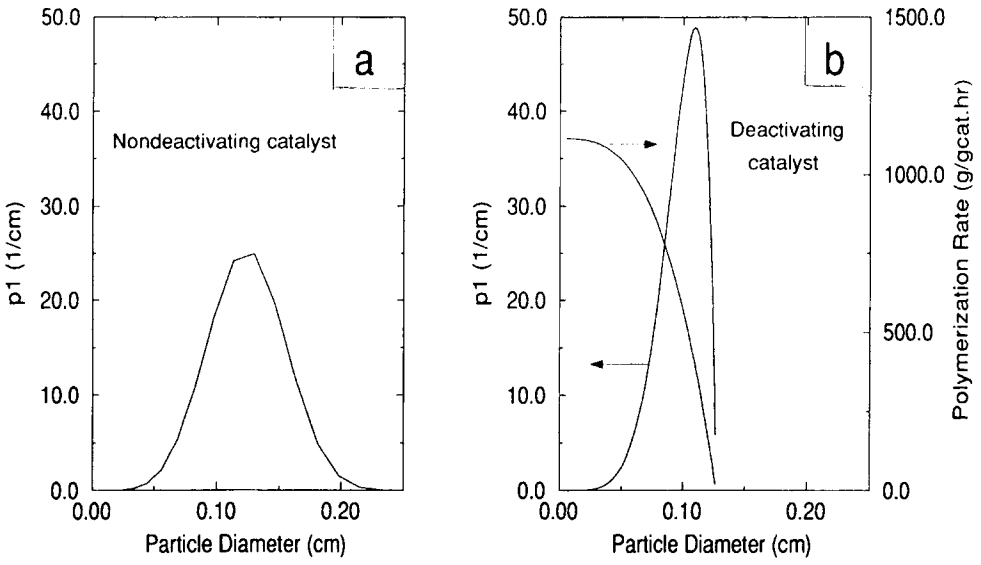

Figure 2 Polymer particle size distribution for nondeactivating and deactivating catalysts with uniform size catalyst feed; deactivation half-life = 8 h.

lyst deactivation half-life is 8 h and the feed catalyst has uniform particle diameter of 50 μm. It is assumed that the site deactivation occurs uniformly following the first order deactivation kinetics. Figure 2 shows that the polymer particle size distribution is bell shaped and nearly symmetric for nondeactivating catalyst with a mean particle diameter of about 1,200 μm. Recall that only a small amount of catalyst particles is injected to the reactor and each catalyst particle grows to larger polymer particles in the reactor. If the polymer particles do not grow from their initial small catalyst particles, such a bell-shaped particle size distribution will not be obtained. This implies that a simple residence time distribution model for a perfectly backmixed homogeneous flow system is not directly applicable to the gas phase polymerization reactor system. When the catalyst site deactivation occurs with a growth of polymer particle, the resulting particle size distribution becomes quite different [Fig. 2(b)] from that for the

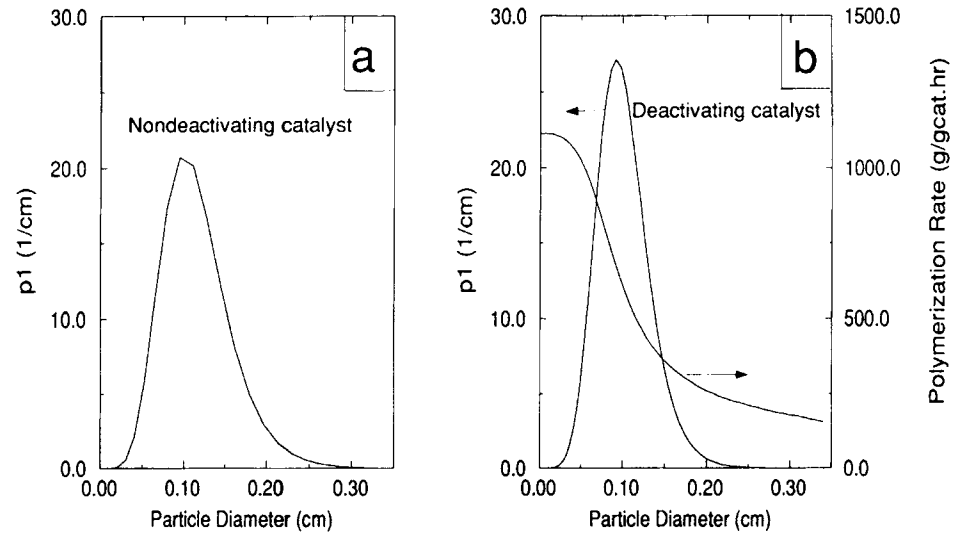

Figure 3 Polymer particle size distribution for nondeactivating and deactivating catalysts with log-normally distributed feed catalyst particles; deactivation half-life = 8 h.

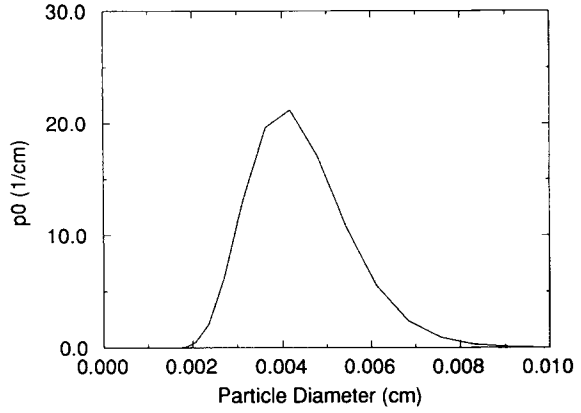

Figure 4 Log-normal feed catalyst particle size distribution.

nondeactivating catalyst case. Notice that the particle size distribution curve is asymmetric and the amount of large polymer particles is far smaller than the case for nondeactivating catalyst. This is because, as indicated in Figure 2(b), the polymerization rate decreases rapidly as the age of a polymer particle increases. The simulation results shown in Figure 2 indicate that one can assess the effect of catalyst deactivation by observing the shape or symmetry of the resulting polymer particle size distribution curves for uniform sized catalyst feed.

The effect of nonuniformly sized catalyst feed is shown in Figure 3. Here, the catalyst feed is assumed to have the following log-normal particle size distribution:

$$p_0(R_c) = \frac{1}{\sqrt{2\pi} R_c \ln \sigma} \exp\left(-\frac{(\ln R_c - \ln \bar{R}_c)^2}{2(\ln \sigma)^2}\right) \quad (16)$$

where R_c is the catalyst particle radius, $\bar{R}_c$ the average catalyst particle radius, and σ the geometric standard deviation. For mean catalyst radius of 25 μm and σ = 1.28 μm, the catalyst particle size distribution is shown in Figure 4. In this case, the effect of catalyst deactivation is also clearly seen in Figure 3(b) that shows that the particle size distribution is narrow with a significantly reduced fraction of large polymer particles. Figure 5 shows the effect of catalyst deactivation parameter (i.e., deactivation half-life) on the polymer particle size distribution and overall polymerization rate for the log-normal catalyst particle size distribution. Again, it is seen that as the catalyst deactivates more rapidly (i.e., smaller deactivation half-life), the average polymer particle size becomes smaller and the polymer particle size distribution becomes narrower because of a decreased fraction of large polymer particles.

In the previous examples, uniform site deactivation has been assumed for all catalytic sites. In such a case, the polymer properties such as polymer molecular weight averages and weight percent comonomer incorporated into the polymer are little affected but the overall polymer production rate decreases. If the site activity changes nonuniformly during the polymerization, it is possible that polymer properties may change as polymer particles grow. For example, we can think of the catalyst sites that lose the ability to incorporate comonomers into the

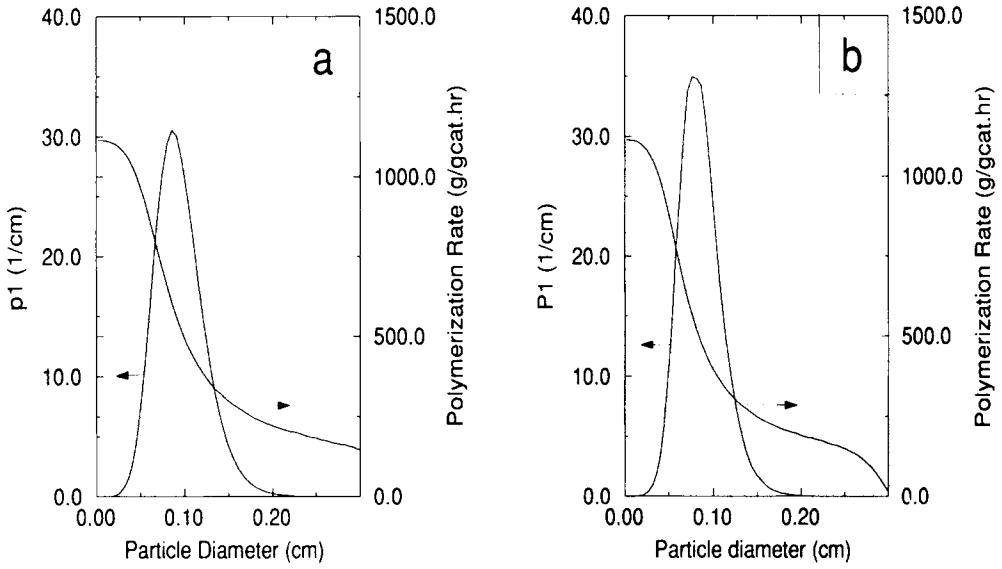

Figure 5 Effect of catalyst deactivation with log-normally distributed catalyst feed size distribution; deactivation half-life (a) 5 h and (b) 8 h.

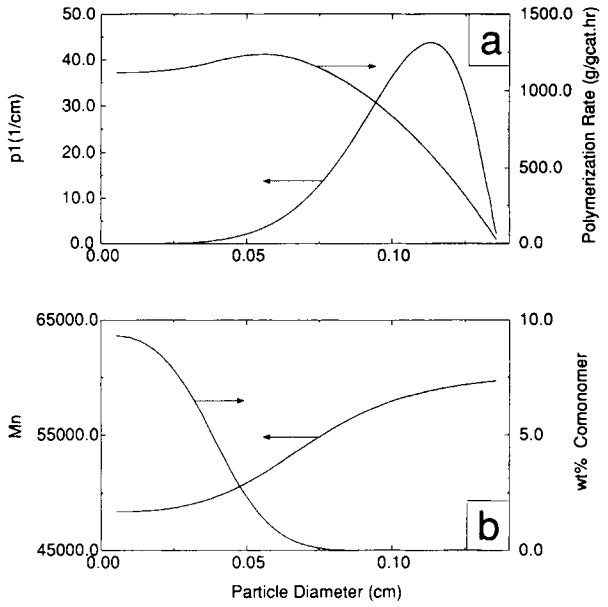

Figure 6 Effect of nonuniform site deactivation: site deactivation half-life = 8 h, copolymerization activity decay rate constant = 1 h^{-1}, uniform sized catalyst feed.

polymer as the residence time or age of the catalyst increases. Figure 6 shows the simulation results for such a case where it is assumed that the overall catalyst deactivation half-life is 8 h but at the same time the catalyst activity toward comonomer declines. Here, the activity of the catalytic sites toward the incorporation of comonomer (i.e., k_{12} and k_{22} values) is assumed to decrease exponentially with particle residence time. Figure 6(a) shows the polymer particle size distribution curve and the polymerization rate profiles for uniform sized catalyst feed. As the catalyst loses its ability to incorporate less reactive comonomer, the overall polymerization rate increases slightly for small particles because more reactive ethylene is perferably polymerized; however, as the particles grow, the site deactivation effect becomes more pronounced and the overall polymerization rate decreases sharply. As a result of nonuniform site deactivation, both polymer molecular weight and the weight percent of comonomer in the polymer phase change significantly as illustrated in Figure 6(b). As less comonomers and relatively larger amounts of ethylene are incorporated into the polymer, polymer molecular weight increases. The content of comonomer in large particles is small, leading to higher polymer density. Note that the weight fraction of comonomer in the particles of size larger than 1,000 μm is almost 0. The simulation results shown in Figure 6 indicate that a significant degree of heterogeneity in polymer properties should be expected for the polymer particles of different size when nonuniform site deactivation occurs. Similar simulations have been carried out for log-normally distributed catalyst feed particles (Fig. 7) and the results are qualitatively very similar to those for uniform sized catalyst feed particles.

The effects of catalyst injection rate, solid bed weight, and deactivation half-life on particle mean residence time defined by Eq. (14) are shown in Figure 8. For a fixed bed weight, the polymer production rate for a rapidly deactivating catalyst (i.e., short half-life) is small and thus the mean residence time becomes large. It is to be noted that in such a case a large amount of "dead" catalyst–polymer particles are present in the reactor. It is also seen for a large catalyst injection rate that the mean residence time is nearly independent of the catalyst deactivation. Similar observations can be made in Figure 8(b) where the catalyst injection rate is fixed but the bed weight is varied.

CONCLUSIONS

In this article we have presented the population balance models for a steady-state gas phase ethylene copolymerization reactor. A MGSCM is incorpo-

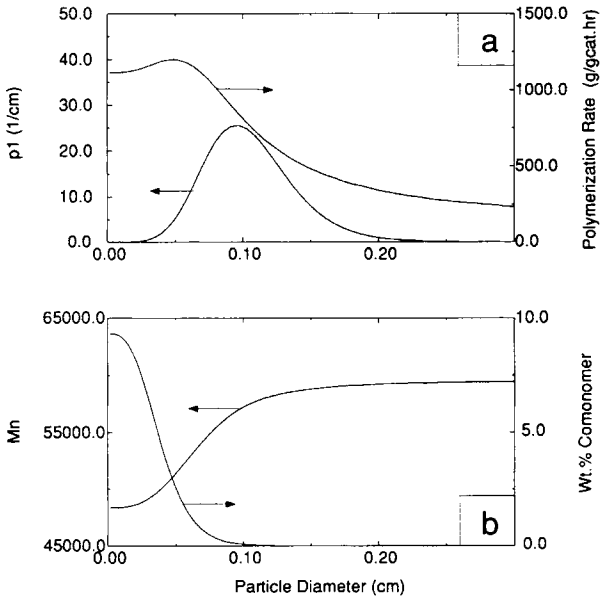

Figure 7 Effect of nonuniform site deactivation for log-normally distributed catalyst feed size distribution: site deactivation half-life = 8 h, copolymerization activity decay rate constant = 1 h^{-1}.

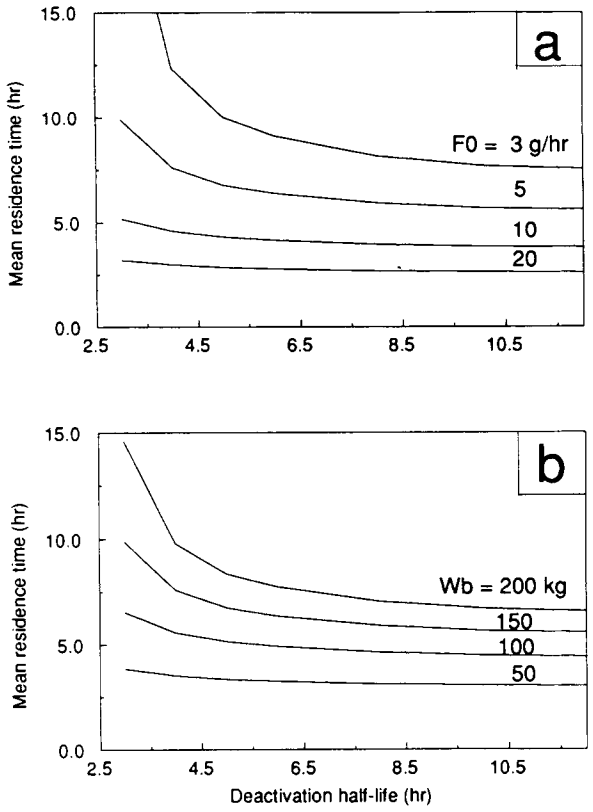

Figure 8 Effect of deactivation half-life on mean residence time: (a) W_b = 150 kg and (b) F_0 = 5.0 g/h.

rated into the population balance model to compute the polymer particle size and polymer properties. The two major effects investigated are the feed catalyst particle size distribution and the catalyst site deactivation. In the presence of site deactivation, the particle size distribution becomes asymmetric with a reduction in the amount of large polymer particles. It has been observed that the polymer particle size distribution becomes narrower as the catalyst deactivation occurs more rapidly. When the site deactivation occurs nonuniformly, the resulting polymer properties depend upon the age or size of the polymer particles. Those phenomena observed in this study through numerical model simulations would be useful in understanding the effect of various catalyst kinetic parameters on the polymer properties in industrial gas phase copolymerization processes.

REFERENCES

1. T. W. Taylor, K. Y. Choi, H. Yuan, and W. H. Ray, *Transition Metal Catalyzed Polymerizations,* R. P. Quirk, Ed., Harwood Academic Publishers, New York, 1983, p. 191.
2. M. Kakugo, H. Sadatoshi, M. Yokoyama, and K. Kojima, *Macromolecules,* **22,** 547 (1989).
3. M. Kakugo, H. Sadatoshi, J. Sakai, and M. Yokoyama, *Macromolecules,* **22,** 3172 (1989).
4. R. A. Hutchinson and W. H. Ray, *J. Appl. Polym. Sci.,* **41,** 51 (1990).
5. D. Kunii and O. Levenspiel, *Fluidization Engineering,* 2nd ed., Butterworth Heinemann, Boston, MA, 1991.
6. X. Zhao, M.S. Thesis, University of Maryland, College Park, MD, 1993.
7. W. H. Ray, *J. Macromol. Sci.-Rev. Macromol. Chem.,* **C8**(1), 1 (1972).

Received January 26, 1994
Accepted March 7, 1994